Liquid light condensates

H. Michinel,[1] J. Campo-Táboas,[1] R. García-Fernández,[1] J. R. Salgueiro,[2] and M. L. Quiroga-Teixeiro[3]

[1]*Area de Optica, Facultade de Ciencias de Ourense, Universidade de Vigo, Campus de As Lagoas s/n, Ourense, ES-32005, Spain*
[2]*Escola Universitaria de Optica e Optometría, Universidade de Santiago de Compostela, Campus Sur s/n, Santiago, ES-15706, Spain*
[3]*Institute for Microelectronics, Department of Optoelectronics, Chalmers University of Technology,*
Goteborg, S-41296 Sweden

We show that a laser beam which propagates through a cubic-quintic nonlinear optical material may reach, for a given power, a condensed state with a collisional dynamics resembling a liquid drop. We qualitatively describe the analogies between this system and the usual fluids and show them by simulating numerically total reflections of these beams with planar boundaries and localized defects. We use the analogy ''liquid light'' to stress the connections with the dynamics of quantum fluids, including Bose-Einstein condensates.

PACS number(s): 42.65.−k

I. INTRODUCTION

If a laser beam is regarded as a gas of photons, two interesting questions can be formulated: Would it be possible to produce something like a state of liquid light? and what physical properties will this peculiar state show? We will demonstrate in the present paper that high-power laser beams and pulses which propagate through certain nonlinear optical materials, may reach a condensed state with physical behavior resembling a (coherent) liquid droplet. We have performed a numerical exploration of the properties of these ''light droplets,'' inspired by the physical picture of the surface tension of the usual liquids. Our numerical simulations reveal that the collisions of light ''streams'' (i.e., laser beams) and droplets (i.e., laser pulsed beams) against boundaries and localized inhomogeneities show interesting analogies with fluid mechanics. The calculations also demonstrate that our theoretical predictions can be tested in the frame of current experiments with realistic materials.

Thus, we will begin by recalling some well-known effects of laser beam propagation in cubic-quintic nonlinear media, which are the simplest optical materials where light condensates can be obtained. Next, we will analyze in detail the peculiar shape of the stationary states of the system and formulate two simple ideal experiments to detect properties of ''light streams'' and ''light droplets'' analogous to the surface tension of liquids. Finally, we performed the numerical implementation of these ideas and found that light condensates do exhibit surface tension properties. We calculated the main parameters involved for realistic materials, in order to stimulate the experimental test of our predictions.

II. PHYSICAL MODEL

Thus, let us begin by recalling some well-known effects concerning nonresonant laser propagation in nonlinear materials. In optical media presenting linear growth of the refractive index shift with light intensity (optical Kerr effect), envelope solitons [1–3] can be produced for one-dimensional propagation. They can be obtained as pulses in optical fibers with anomalous dispersion (temporal solitons) or as continuous beams in several planar configurations. On the other hand, wild unstable phenomena like blowup and catastrophic self-focusing take place for intense two-dimensional propagation in bulk Kerr-like materials [4]. However, collapse can be limited if the nonlinear growth of the refractive index saturates for high powers, and thus stable two-dimensional stationary beams can be obtained [5,6].

In the present work, we will analyze the dynamical properties of laser beams and pulses propagating through a nonlinear optical material with the following refractive index:

$$n(I) = n_0 + n_2 I - n_4 I^2, \qquad (1)$$

where n_0, n_2, and n_4 are positive constants determining the nonlinear response of the optical material with the intensity (I) of the light beam. This kind of refractive index represents the so-called cubic-quintic optical materials [7–11] and it can be considered as a Taylor expansion up to I^2 terms of more complicated optical nonlinearities. The above $n(I)$ grows with increasing I for low powers, and diminishes for high powers due to the contribution of the negative $n_4 I^2$ term. Very interesting examples of materials that correspond to the refractive index of Eq. (1) are the recently reported
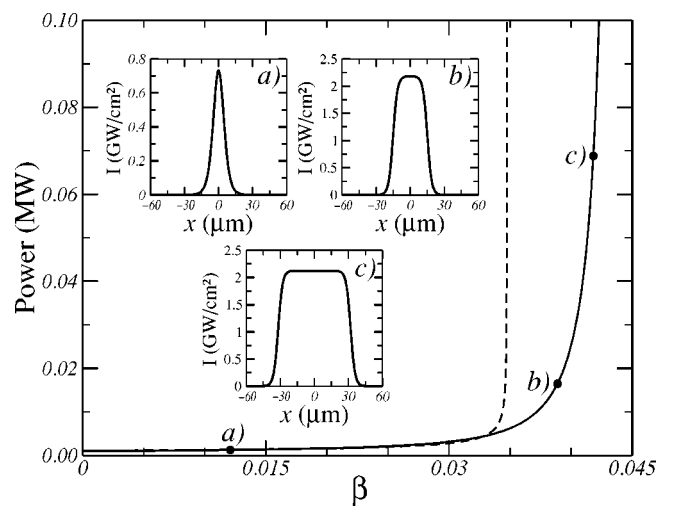

FIG. 1. Beam power (N) vs nonlinear phase shift (β) for stationary nodeless states. Solid line, numerical; dashed line, variational. Note that the power grows monotonically with β and there is a gap (N_0) at $\beta = 0$. Insets: beam shapes corresponding to several values of power. Note that the intensity scale at (a) is different.
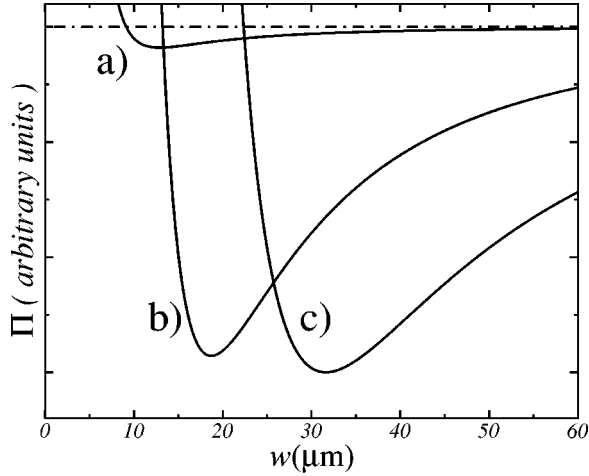
FIG. 2. Potential functions given by Eq. (4) of the nodeless states (a), (b), and (c) from Fig. 1.

nonlinearities of chalcogenide glasses [12], which show an intensity-dependent refractive index that can be fitted by Eq. (1). Our aim in the present paper will be to show that this change in the sign of the nonlinear response with the intensity leads to the formation of light condensates with physical properties resembling those of fluids. These light condensates can be obtained in the form of continuous or pulsed beams. Thus, we will use the terms *light streams* and *light drops*, respectively, to refer to each case.

We will analyze in the first place the propagation along z, in the paraxial regime, of a continuous linearly polarized laser beam trough a nonlinear optical material with the above refractive index $n(I)$. The dynamics of the envelope of the electromagnetic wave $\Psi(x,y,z)$ is given by a generalized nonlinear Schrödinger equation (NLSE) of the form [7]

$$2ikn_0\frac{\partial\Psi}{\partial z}+\nabla_\perp^2\Psi+2k^2n_0(n_2|\Psi|^2-n_4|\Psi|^4)\Psi=0, \quad (2)$$

where $k=2\pi/\lambda$ is the wave number in vacuum and $\nabla_\perp^2=\partial^2/\partial x^2+\partial^2/\partial y^2$. Typical values of the above parameters
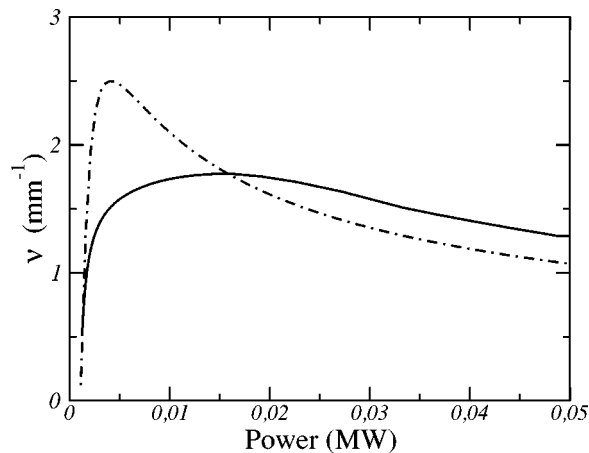

FIG. 3. Resonance frequencies (ν) of the nodeless states as a function of the beam power. Dashed (solid) lines correspond to variational (numerical) calculations, as given by Eq. (7).
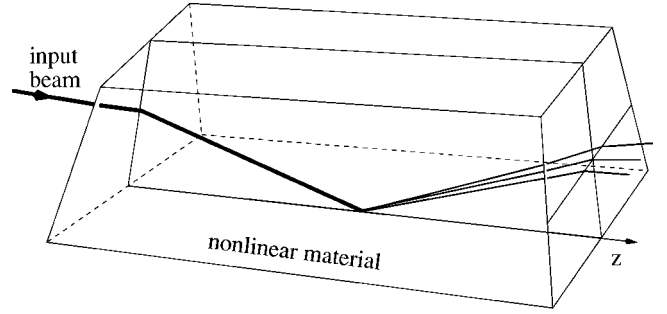

FIG. 4. Sketch of the numerical simulation of Fig. 5, showing total reflection at a nonlinear-linear interface.

can be chosen to fit the usual experimental configurations by taking $n_0=1.8$, $n_2\approx2\times10^{-3}$ cm^2/GW, and $n_4\approx2\times10^{-4}$ cm^4/GW^2, with $\lambda=1600$ nm. Thus, nonlinear effects become significant for values of I in the range of GW/cm^2. The physical picture of the above nonlinearity is evident: for low intensities, propagation remains in a quasi-linear regime. If the power is increased, nonlinear self-focusing tends to counteract diffraction and will overcome it for a critical beam flux. This would yield to blowup in pure Kerr materials ($n_4=0$). However, for high powers, the defocusing effect of the term n_4I^2 will balance collapse, yielding a stable two-dimensional beam.

III. STATIONARY NODELESS STATES

Before analyzing the dynamics of laser beams, it is useful to take a look at the spatial profile of the lowest-order stationary solutions of Eq. (2), which are nodeless wave functions of the form $\Psi=\psi(r)e^{i\beta z}$, where β is the nonlinear phase shift (propagation constant) and $\Psi(\infty)=0$. It can be seen in Fig. 1 that the shape and properties of the above states depend crucially on the value of β. In contrast to linear waveguides (where there is only one fundamental mode with a given β) nonlinear propagation yields a continuum of nodeless eigenstates. This is evident, since the nonlinear beam generates its own waveguide during propagation. Thus, we have found by numerical integration the stationary states corresponding to Eq. (2) for increasing values of the nonlinear phase shift, starting from $\beta=0$. The result is a continuum of stationary states with different shapes and increasing values of the beam power $N=\int|\Psi|^2dxdy$. Some of these spatial profiles are shown in the insets of Fig. 1.

The form of the stationary solutions of Eq. (2) has been analyzed by several authors [13–15]. It is well known, for instance, that there is a minimum power threshold N_0 to generate a stationary beam. Obviously, this minimum beam flux coincides with the collapse power threshold for a Gaussian beam in bulk Kerr media [16,17]. We must also point out that there is a critical value β_c of the propagation constant for which N diverges. Thus, for $\beta>\beta_c$, no stationary solutions can be obtained. Although there are good analytical approximations for the shapes of previous stationary beams [15], less attention has been paid to investigating the peculiar form of the spatial profiles of Fig. 1 from a physical point of view. Thus, let us try to extract a qualitative picture of the
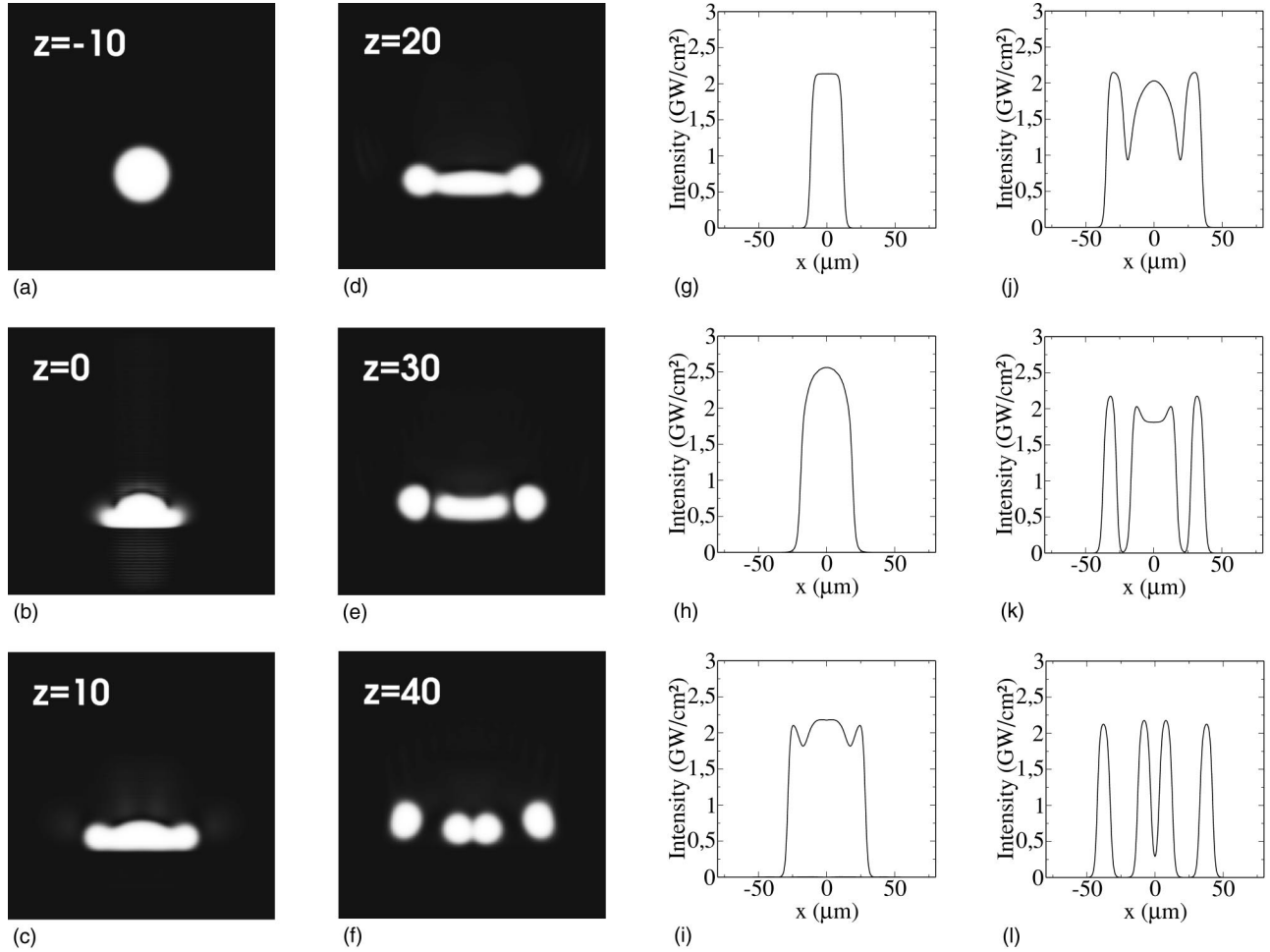
FIG. 5. Numerical simulation corresponding to the sketch of Fig. 4. (a)–(f) Gray scale images of the transverse xy plane for different values of z (in μm). (g)–(l) Maximum intensity profiles along the x axis corresponding to the above gray scale images. The scale of the x axis is the same in both top and bottom pictures.

properties of the mentioned stationary beams, by analyzing the changes in the shape of the eigenstates of Eq. (2) for growing values of β.

As can be appreciated in Fig. 1, low values of the beam flux N (i.e., $\beta \rightarrow 0$) lead to light distributions with quasi-Gaussian profiles. As β is increased, the beam flux grows and the spatial shapes tend to narrow, approximately keeping the Gaussian shape and reaching a minimum width and a maximum peak for an intermediate power. For larger values of β, the beam flux grows rapidly and the peak intensity of the light distribution saturates due to the effect of n_4. The light distributions tend to super-Gaussian profiles and thus *high-power stationary beams yield wide flat-topped profiles.* The slope at half maximum grows with the power and tends to a maximum constant value, with the result that the shapes of high-power beams differ only in the length of the flat top. If we reconsider the previous scenario in the light of the statistical mechanics of a "photon gas," it resembles a phase transition from a gas cloud into a liquid drop. The analogy would be as follows. In Eq. (2) the diffraction ($\nabla^2 \psi$) can be interpreted as a kinetic term (thermal expansion of the photon gas) and the nonlinearity can be regarded as a "cooling effect," opposed to the kinetic term $\nabla^2 \psi$. Stable "light

streams" are formed due to the competing effects of diffraction, the Kerr term (n_2), and the self-defocusing nonlinearity (n_4), similar to the way van der Waals forces form liquid droplets in gas-liquid condensation. Thus, low-power beams (i.e., $\beta \rightarrow 0$, quasilinear regime) yield to Gaussian-like spatial distributions with boundaries less sharp than in the case of high-power beams, where the distributions are close to super-Gaussian functions. The analogy is more evident in the case of pulsed beams, where "light droplets" will be obtained. We will analyze this case in the last section of the present work.

Thus, if one assumes the previous picture, the next step is to formulate ideal experiments to detect the typical behavior of liquids in the liquid light states mentioned, like the existence of properties resembling surface tension.

IV. SMALL AMPLITUDE OSCILLATIONS

To get a deeper physical insight into the properties of the above light distributions, we performed a variational analysis of the frequency spectrum of the small amplitude oscillations of slightly perturbed stationary beams. The perturbation can be experimentally implemented with a thin lens, which adds
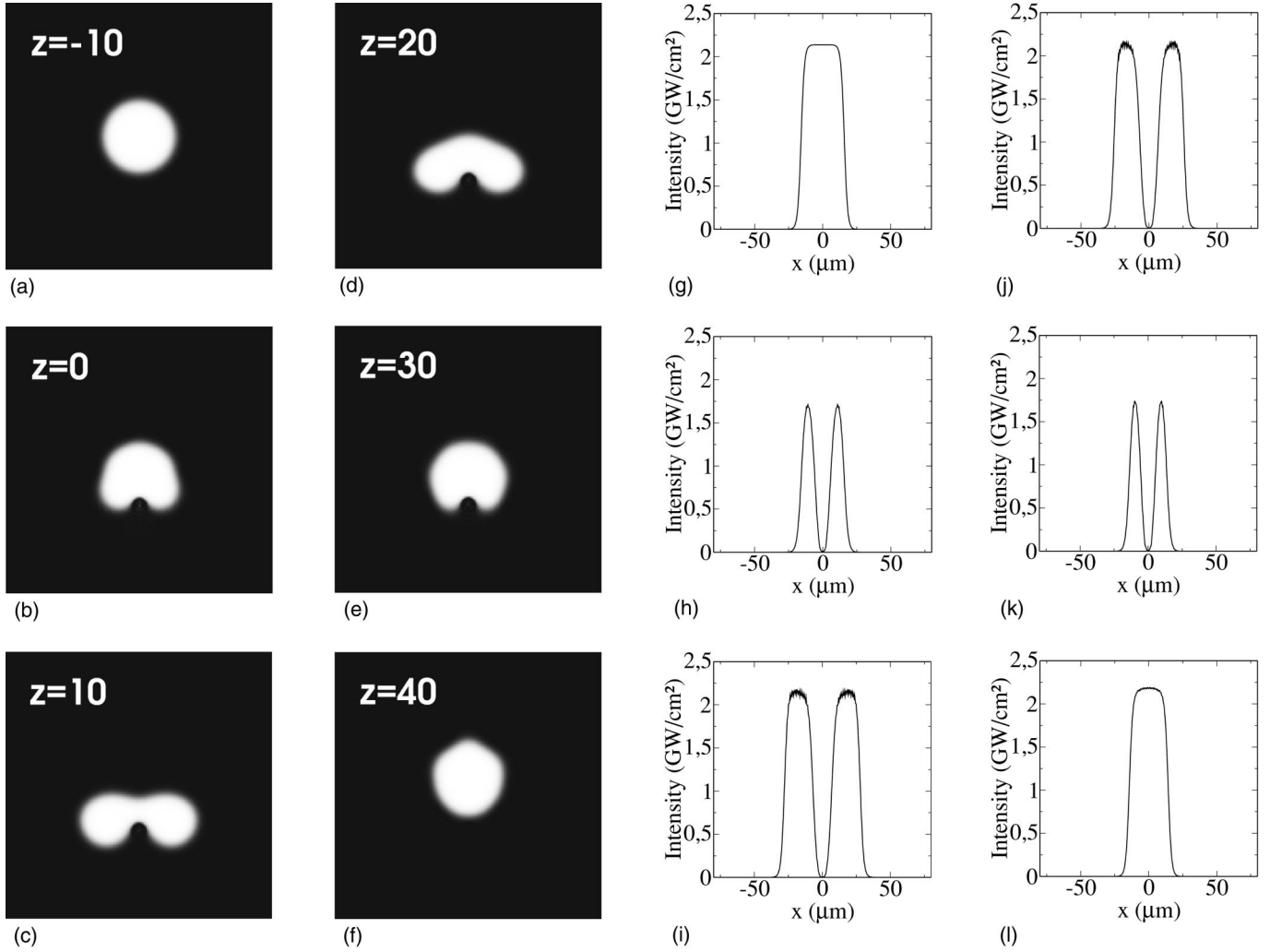
FIG. 6. The same as Fig. 5 for total reflection at an 8 μm air hole.

a slight curvature to an input Gaussian beam. As we will show, the beam will oscillate periodically like an elastic material forced with an instantaneous perturbation. Thus, the frequency of the oscillations can be considered as a measurement of the rigidity of the stationary state. The variational approach [13,14,18] starts by describing the evolution of the beam by means of the following trial function:

$$\Psi(r,z) = \psi(z)\exp\left[-\frac{r^2}{2w^2(z)} + ib(z)r^2\right], \quad (3)$$

where ψ, w, and b are quantities depending on z, corresponding to the peak amplitude, beam width and curvature, respectively. Following the standard variational procedure, after minimization of the corresponding Lagrangian density over the set of trial functions from Eq. (3), an ordinary Newton-like differential equation is obtained for the above parameter w. These equations can be reformulated in terms of effective potentials for equivalent particles in the following form [14]:

$$\Pi = \left(\frac{1}{k^2 n_0^2} - \frac{n_2 N}{2\pi n_0}\right)w^{-2} + \frac{2n_4 N^2}{9\pi^2 n_0}w^{-4}. \quad (4)$$

The widths of the perturbed beams evolve, oscillating around the minimum of Π, like classical particles in potential wells, z playing the role of time. In Fig. 2, we plot the shapes of the previous potentials for three different values of the peak power, corresponding to the shapes of the insets in Fig. 1. As can be seen in the plot, the higher N, the deeper Π. The minimum width of the potential is achieved for the (b) eigenstate. The variational analysis, although not exact, provides the widths of the stationary states w_s as a function of the beam power. They are given by the values of w for which Π is minimum. From a simple inspection of Eq. (4) the following value for the width of the beam is obtained:

$$w_s^2 = \frac{8n_4}{9n_2}\frac{N^2}{N-N_0}, \quad (5)$$

where N_0 is the critical value for the beam flux,

$$N_0 = \frac{2\pi}{k^2 n_0 n_2}. \quad (6)$$

The value of N_0 is the small gap in the beam power at $\beta = 0$ of Fig. 1. It is straightforward to calculate the minimum width w_m of a stationary beam, which is achieved for $N = 2N_0$ and is given by $w_m = (8/3kn_2)\sqrt{\pi n_4/n_0}$. For the experimental values given above, it is easily obtained that $w_m \approx 6.4$ μm, which gives peak powers in the range of 2 GW/cm^2 to generate the stationary states. Thus, the variational model predicts a minimum beam power to generate the stationary states that we numerically calculated above. Obviously, Eq. (6) coincides with the critical collapse threshold for a Gaussian beam in a bulk Kerr material [17]. The comparison with direct numerical calculations, as can be appreciated in Fig. 1, gives very good agreement (error below 1%) for low values of β. However, it must be stressed that, as the shape of the stationary states deviates from the Gaussian profile, the fit of the theoretical and numerical curves is only qualitative.

In the second place, notice that by expanding Π around its minimum it is possible to obtain the frequencies ν of small amplitude oscillations along z of perturbed stationary states, as functions of the main parameters involved, and thus the beams will behave as harmonic oscillators. Therefore, to get a more physical picture of the light condensates, it is interesting to consider ν as a measure of the "rigidity" of the oscillators corresponding to the different stationary states. Hence, after a simple Taylor expansion around the minimum of Π, we obtain

$$\nu = \frac{9\pi}{4\sqrt{2}k^3 n_0^2 n_4} \frac{(N/N_0 - 1)^{3/2}}{N^2}. \tag{7}$$

In Fig. 3, we show a comparison between the variational formula (7) and the numerically calculated frequencies for the different eigenstates of the system. To carry out this calculation, we have added a small curvature to each eigenstate of the system, propagated them, and performed the Fourier transform of the amplitude oscillations. The variational analysis reveals that a maximum rigidity of the light condensate is achieved for a given value of N (or equivalently β). The critical value of N corresponding to the maximum frequency can be easily calculated by taking $d\nu/dN = 0$, and is given by

$$N_{cr} = \frac{8\pi}{k^2 n_0 n_2} = 4N_0. \tag{8}$$

In Fig. 3, we observe that the variational method has only a qualitative agreement with the numerical (solid line) calculation. We can argue that N_{cr} is a critical value for the behavior of the beams at total reflection. Over this value of N, the stationary states become flat topped and thus the light distributions will show a constant density of photons around the center of the beam, and a sharp decay at the boundary. These beams will show a higher stability against small perturbations at the boundary. This can be qualitatively understood by taking into account the fluid picture mentioned above. If one considers that a gas-liquid phase transition is taking place as the power is increased, the maximum rigidity
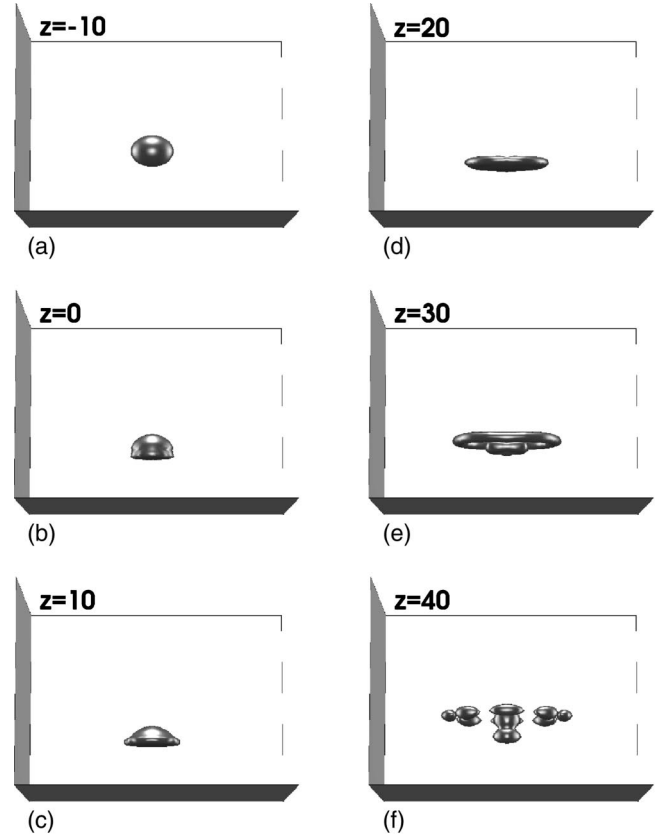

FIG. 7. Numerical simulation of the collision of a light drop against a planar boundary (not visible in the graphs). The values of z in each picture are the distance of the center of the pulse to the origin of coordinates. The paper plane is xy and z is perpendicular to the paper plane. The experimental parameters are given in the text.

will establish the gas-liquid frontier above which beams will have some kind of surface tension that can block the emission of radiation at total reflection of the beam.

V. NUMERICAL SIMULATIONS

In the present section we analyze numerically the propagation of a light condensate through a bulk cubic-quintic nonlinear optical material in the presence of boundary conditions and localized inhomogeneities (holes). The propagation equation for the above waveguide in the paraxial regime is a generalized NLSE, including the effect of boundaries or holes. The experimental parameters are in the same range as in the previous sections.

Our computer simulations show that there is a deep analogy between incompressible fluid dynamics and the interference behavior of light condensates at boundaries and localized discontinuities. This can be understood by thinking of light condensates as having some kind of "surface tension," analogous to that of a liquid droplet. Considering that diffraction in the NLSE plays the role of a kinetic energy term, a Kerr-like material can be regarded as a "cold medium" that tends to compress the photon gas (i.e., beam self-focusing). From this point of view, when collapse is stopped due to

quintic defocusing terms, the situation is similar to droplet condensation due to van der Waals forces.

As in the case of liquids, one can expect surface tension properties from the resulting light condensates. To show this, we present two particular cases from our numerical investigation. Both simulations correspond to a radial stationary fundamental state of the propagation equation. The beam is 25 μm wide and its peak intensity is 2.0 GW/cm^2.

The numerical simulations were performed with standard Fourier beam propagation method in a 1024-point grid. In Fig. 4, we show a sketch of the numerical calculations of Fig. 5, where we have simulated internal reflection inside a bulk cubic-quintic material surrounded by air. This can be done by adding to Eq. (2) a term $2k^2 n_0 \Delta n(x,y)\Psi$, $n_0 + \Delta n$ being the linear refractive index of the nonlinear material. To simulate total reflection at a planar interface between the nonlinear material and air, we chose $n_0 = 1.0$ and $\Delta n = 0.8$ for the half plane $x > 0$ and $\Delta n = 0$ for $x \leq 0$. The interference pattern when the beam reaches the boundary clearly resembles crushing of a liquid drop thrown toward a solid wall which splits into smaller droplets. We have performed a large series of numerical explorations for different angles of incidence, from the quasielastic to the complete inelastic range, showing that the surface tension effect provides the beam with a high stability.

In Fig. 6 we plotted a collision with an 8 μm air hole immersed in the bulk nonlinear material. In this case, we use $\Delta n = 0.8$ inside a circle of 8 μm radius and $\Delta n = 0$ outside it. The rest of the parameters are set equal to the previous simulation. The effect is analogous to that of a surface tension: The beam is strangulated when it intersects the hole. However, it recovers its original form if the angle of incidence is below a critical value. Both simulations show that light condensates behave in a similar fashion to liquids against collisional perturbations. The analogy with surface tension properties can be qualitatively understood as a balance between the radiation pressure inside and outside the beam. Inside the beam, the refractive index is greater than outside, due to the nonlinear effects. However, a detailed understanding of the phenomenon should start from a thermodynamical point of view, defining quantitative concepts like the temperature and entropy of the beams for a given nonlinearity. This is a deep problem that we leave to further research.

VI. PULSED BEAMS

If the beam is pulsed, time must be included in the simulations. Thus, an extra second derivative with respect to "proper time" should be added to Eq. (2) in order to take into account the effect of second-order dispersion. The corresponding NLSE becomes $1+3$ dimensional, and extra difficulties are added to the numerical simulations. Not only is the increase in the length of the calculations inconvenient but so is the representation of the data obtained. The need for analytical tools like the variational model is more evident in this case.

Thus, taking into account the data obtained for the two-dimensional case of laser beams, we will analyze the properties of pulsed beams, which propagate in cubic-quintic materials, corresponding to the same material parameters as in the previous cases. The result is plotted in Fig. 7, where we have simulated the total reflection of a pulsed beam for the case of anomalous dispersion. It can be seen that the effect of the planar boundary between the nonlinear and the linear material (not shown in the pictures) is to generate a corona of droplets in a similar way as happens in the crushing of a liquid drop. In fact, the dominant effect in the generation of smaller pulses at the boundary is modulational instability [6,19–22] around the rings formed by diffraction.

We must note the deep connection of this case with the dynamics of Bose-Einstein condensates (BECs) in alkali-metal gases. In fact, the collective dynamics of a BEC in the absence of a trapping potential is given by a NLSE which is usually called the Gross-Pitaevskii equation:

$$i\hbar \frac{\partial \Psi}{\partial t} + \frac{\hbar^2}{2m}\nabla^2\Psi + c_1|\Psi|^2\Psi - c_2|\Psi|^4\Psi = 0, \qquad (9)$$

where Ψ is the wave function of the condensate and c_1 and c_2 are positive constants describing, respectively, the effect of a negative scattering length and repulsive three-body elastic interactions. The previous equation for the coherent cloud is formally the same as Eq. (2). Thus, it is evident that similar behavior as shown in Fig. 7 could be expected for BECs with an adequate experimental configuration. In fact, the possibility of gas-liquid phase transitions in Bose-Einstein condensates has recently been put forward by several authors [23]. This means that for dense enough BECs one could expect a phase transition from a gas cloud to a (coherent) liquid drop.

VII. CONCLUSIONS

In the present work we described the phenomenon of light condensation in nonlinear optical materials with cubic-quintic nonlinearity. To support the analogy between light condensates and liquids, we tested the surface tension properties of "light streams" and "light drops" by simulating collisions against planar boundaries and localized inhomogeneities. Our predictions are fully verifiable in the frame of current experiments and open interesting connections between nonlinear optics and the dynamics of quantum fluids, including Bose-Einstein condensates.

[1] A.W. Snyder and D.J. Mitchell, Science **276**, 1538 (1997).

[2] G.I. Stegeman and M. Segev, Science **286**, 1518 (1999).

[3] *Optical Solitons: Theoretical Challenges and Industrial Perspectives,* edited by V. E. Zakharov and S. Wabnitz (Springer-Verlag, Berlin, 1999).

[4] *Wave Collapse,* edited by E. Kutnetsov, A. Zakharov, and E. Vladimir (World Scientific, Singapore, 1999); C. Sulem and P. L. Sulem, *The Nonlinear Schrödinger Equation: Self-Focusing and Wave Collapse* (Springer-Verlag, Berlin, 1999).

[5] Y. Silberberg, Opt. Lett. **15**, 1282 (1990).

[6] N.N. Akhmediev, D.R. Heatley, G.I. Stegeman, and E.M. Wright, Phys. Rev. Lett. **65**, 1423 (1990).

[7] A.H. Piekara, J.S. Moore, and M.S. Feld, Phys. Rev. A **9**, 1403 (1974).

[8] D.E. Edmundson and R.H. Enns, Phys. Rev. A **51**, 2491 (1995).

[9] C. Josserand and S. Rica, Phys. Rev. Lett. **78**, 1215 (1997).

[10] R. McLeod, K. Wagner, and S. Blair, Phys. Rev. A **52**, 3254 (1995).

[11] Z. Jovanoski, J. Mod. Opt. **48**, 865 (2001).

[12] F. Smektala, C. Quemard, V. Couderc, and A. Barthelemy, J. Non-Cryst. Solids **274**, 232 (2000).

[13] M. Quiroga-Teixeiro and H. Michinel, J. Opt. Soc. Am. B **14**, 2004 (1997).

[14] M. Quiroga-Teixeiro, A. Berntson, and H. Michinel, J. Opt. Soc. Am. B **16**, 1697 (1999).

[15] K. Dimitrievski, E. Reimhult, E. Svensson, A. Öhgren, D. Anderson, A. Berntson, M. Lisak, and M.L. Quiroga-Teixeiro, Phys. Lett. A **248**, 369 (1998).

[16] V.I. Bespalov and V.I. Talanov, Zh. Eksp. Teor. Fiz. Pis'ma Red. **3**, 471 (1966).

[17] A.J. Campillo, S.L. Shapiro, and B.R. Suydam Phys. Rev. Lett. **23**, 628 (1973).

[18] D. Anderson, Phys. Rev. A **27**, 3135 (1983).

[19] N.G. Vakhitov and A.A. Kolokolov, Izv. Vyssh. Uchebn. Zaved., Radiofiz. **16**, 1020 (1973).

[20] A.A. Kolokolov, Izv. Vyssh. Uchebn. Zaved., Radiofiz. **17**, 1332 (1974).

[21] J.M. Soto-Crespo, D.R. Heatley, E.M. Wright, and N.N. Akhmediev, Phys. Rev. A **44**, 636 (1991).

[22] N.B. Abraham and W.J. Firth, J. Opt. Soc. Am. B **7**, 951 (1990).

[23] A. Gammal, T. Frederico, L. Tomio, and P. Chomaz, Phys. Rev. A **61**, 051602 (2000)